

José Trincão,^{a,†} Marta Sousa
Silva,^{b,†} Lúcia Barata,^{a,b}
Cecília Bonifácio,^a Sandra
Carvalho,^{c,d} Ana Maria Tomás,^{c,d}
António E. N. Ferreira,^b Carlos
Cordeiro,^b Ana Ponces Freire^b
and Maria João Romão^{a*}

^aREQUIMTE-CQFB, Departamento Química,
Faculdade de Ciências e Tecnologia,
Universidade Nova de Lisboa, Caparica,
Portugal, ^bCentro de Química e Bioquímica,
Departamento Química e Bioquímica,
Faculdade de Ciências da Universidade de
Lisboa, Edifício C8, Lisboa, Portugal,
^cIBMC – Instituto de Biologia Molecular e
Celular, Universidade do Porto, Porto, Portugal,
and ^dICBAS – Instituto de Ciências Biomédicas
Abel Salazar, Universidade do Porto, Porto,
Portugal

† These authors contributed equally to this
work.

Correspondence e-mail: mromao@dq.fct.unl.pt

Received 12 June 2006

Accepted 17 July 2006

Purification, crystallization and preliminary X-ray diffraction analysis of the glyoxalase II from *Leishmania infantum*

In trypanosomatids, trypanothione replaces glutathione in all glutathione-dependent processes. Of the two enzymes involved in the glyoxalase pathway, glyoxalase I and glyoxalase II, the latter shows absolute specificity towards trypanothione thioester, making this enzyme an excellent model to understand the molecular basis of trypanothione binding. Cloned glyoxalase II from *Leishmania infantum* was overexpressed in *Escherichia coli*, purified and crystallized. Crystals belong to space group $C222_1$ (unit-cell parameters $a = 65.6$, $b = 88.3$, $c = 85.2$ Å) and diffract beyond 2.15 Å using synchrotron radiation. The structure was solved by molecular replacement using the human glyoxalase II structure as a search model. These results, together with future detailed kinetic characterization using lactoyltrypanothione, should shed light on the evolutionary selection of trypanothione instead of glutathione by trypanosomatids.

1. Introduction

Trypanosomatids, the causal agents of several human and animal diseases worldwide, present two characteristics that set them apart from all other living organisms. Firstly, glycolysis, the most fundamental biochemical pathway, occurs in these organisms within a specific organelle, the glycosome (Hannaert *et al.*, 2003). Secondly, the unique thiol N^1, N^8 -bis(glutathionyl)spermidine (trypanothione) replaces glutathione in similar eukaryotic glutathione-dependent reactions (Muller *et al.*, 2003; Fairlamb & Cerami, 1992). These differences may be exploited in the development of novel therapeutic strategies, considering that diseases caused by trypanosomatids have no effective curative therapies and are often lethal. Synergistic effects of simultaneous inhibition of multiple trypanothione-dependent enzymes might prove to be the best option, given the absolute need for this thiol during the life cycle of the parasite (Oza *et al.*, 2003).

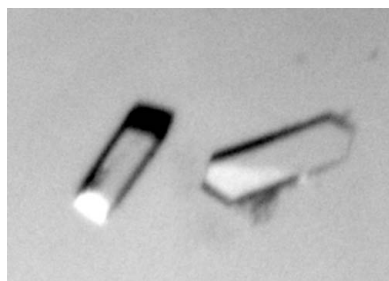
The glyoxalase pathway is one of the important systems that depend on trypanothione. In trypanosomatids, this system is composed of the two enzymes glyoxalase I (lactoylglutathione lyase; EC 4.4.1.5) and glyoxalase II (hydroxyacylglutathione hydrolase; EC 3.1.2.6), which are specific for trypanothione and lactoyltrypanothione, respectively (Sousa Silva *et al.*, 2005; Irsch & Krauth-Siegel, 2004). Glyoxalase II shows absolute specificity towards trypanothione thioester, in contrast to glyoxalase I, which can also react with glutathione-methylglyoxal hemithioacetal (Sousa Silva *et al.*, 2005). Thus, it is an excellent model to understand the molecular basis of trypanothione specificity.

L. infantum glyoxalase II is a monomeric protein with 295 residues (molecular weight 32.5 kDa) and shares 35% homology with the human glutathione-dependent glyoxalase II (Cameron *et al.*, 1999). Here, we report the purification, crystallization and preliminary X-ray diffraction analysis of *L. infantum* glyoxalase II. Its structure determination will shed some light onto the structure–function relationships of the trypanothione-dependent glyoxalase II.

2. Materials and methods

2.1. Cloning, expression and purification

The *LiGLO2* gene was amplified from *L. infantum* (clone MHOM/MA67ITMAP263) genomic DNA. The PCR product was cloned into



the *NdeI/XhoI*-digested expression vector pET-28a (Novagen), which was then transformed into *Escherichia coli* BL21-Codon Plus (Stratagene). For overexpression of His₆-glyoxalase II, BL21-Codon Plus transformants were grown in LB medium containing 50 µg ml⁻¹ kanamycin and 100 µg ml⁻¹ chloramphenicol at 310 K. When the culture reached an OD_{600 nm} of 0.6, expression was induced with 0.2 mM isopropyl β-D-thiogalactopyranoside (IPTG) for 3 h at 310 K. The fusion protein, with an N-terminal tail of six histidines and a thrombin cleavage site (the total tag sequence including linker and cleavage site is HHHHHHSSGLVPRGSH), was purified at 277 K by chromatography on a His-Bind resin (Novagen) column. His₆-LiGLO II was eluted with an imidazole gradient from 5 mM to 1 M at a flow rate of 2.5 ml min⁻¹. Fractions containing glyoxalase II (confirmed by SDS-PAGE) were pooled and the buffer was exchanged to 1 × PBS pH 7.4 using PD-10 columns (Amersham Biosciences). The purity of the recombinant glyoxalase II was estimated by SDS-PAGE. The His₆-LiGLO II was concentrated to 25 mg ml⁻¹ in 10 mM HEPES pH 7.0 using Amicon Ultra-4 filters (10 000 NMWL; Millipore Corporation).

2.2. Crystallization

Crystallization conditions were obtained with an in-house screen of 80 conditions at 293 K, applying the hanging-drop vapour-diffusion method using the crystallization tools from Nextal Biotechnology. Drops were prepared by mixing 2 µl protein solution with 2 µl of each precipitant solution equilibrated over 700 µl reservoir solution. Several conditions in the crystallization screen produced crystals. Crystals were obtained from various conditions including PEGs of molecular weight ranging from 400 to 8000, MES or MOPS with pH between 5.5 and 7.0 and sodium or ammonium acetate as salt components. The best crystals were obtained by mixing 1 µl protein solution with 2 µl reservoir solution containing 30% (w/v) PEG 8000, 0.2 M magnesium chloride and 0.1 M sodium acetate buffer pH 5.5. This final crystallization condition resulted in thick plates, which grew within 2 d to maximum dimensions of approximately 0.16 × 0.06 × 0.02 mm at 288 K (Fig. 1).

2.3. Data collection and processing

Crystals were directly flash-cooled in the cryostream without any additional cryoprotectant. All data were collected at 100 K. A low-resolution data set was collected in-house using a Cu Kα Enraf-Nonius rotating-anode generator operated at 5 kW and a MAR Research image-plate detector (Table 1). A high-resolution native data set was measured at beamline ID14-1 at the European

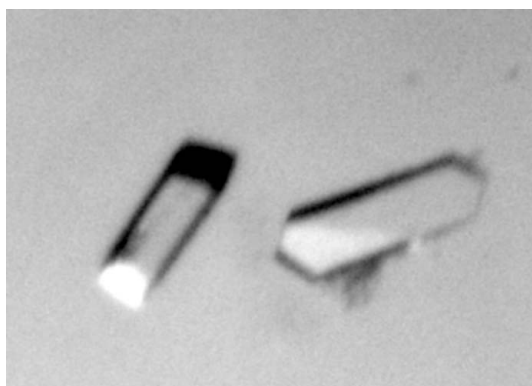


Figure 1
Crystals of *L. infantum* glyoxalase II.

Table 1

Crystal data and data-collection statistics.

Values in parentheses are for the highest resolution shell.

Data set	In-house	ESRF
Space group	C222 ₁	
Unit-cell parameters (Å)	<i>a</i> = 66.6, <i>b</i> = 90.1, <i>c</i> = 85.8	<i>a</i> = 65.6, <i>b</i> = 88.3, <i>c</i> = 85.2
Source	In-house Cu Kα	ID14-1
Wavelength (Å)	1.542	0.934
No. of observed reflections	170772	209900
No. of unique reflections	7294	13574
Resolution limits (Å)	30.0–2.7 (2.85–2.7)	30.0–2.15 (2.27–2.15)
Redundancy	6.0 (5.7)	5.4 (5.2)
R _{sym} † (%)	14.2 (47.7)	10.6 (42.5)
Completeness (%)	99.9 (99.9)	98.4 (98.4)
⟨I/σ(I)⟩	5.3 (1.6)	5.7 (1.7)

† $R_{\text{sym}} = \sum_{\mathbf{h}} \sum_l |I_{\mathbf{h}l} - \langle I_{\mathbf{h}} \rangle| / \sum_{\mathbf{h}} \sum_l I_{\mathbf{h}l}$, where I_l is the l th observation of reflection \mathbf{h} and $\langle I_{\mathbf{h}} \rangle$ is the weighted average intensity for all observations l of reflection \mathbf{h} .

Synchrotron Radiation Facility (ESRF) in Grenoble (France) using an ADSC Quantum 4R CCD detector. The crystal diffracted beyond 2.15 Å.

The diffraction experiments showed that glyoxalase II crystals belong to space group C222₁, with unit-cell parameters *a* = 65.7, *b* = 88.3, *c* = 85.2 Å.

The data were processed using *MOSFLM* v.6.2.5 (Leslie, 1992) and scaled using *SCALA* from the *CCP4* program package v.6.0 (Collaborative Computational Project, Number 4, 1994). In order to estimate the protein content of the asymmetric unit, the Matthews coefficient *V_M* (Matthews, 1968) and solvent content were calculated based on a subunit molecular weight of 32.5 kDa (predicted from the sequence). The structure was solved by molecular replacement using the full structure of the human homologue (PDB code 1qh3; after removing all non-protein atoms) as a search model and the program *Phaser* (Read, 2001) from the *CCP4* suite.

3. Results and discussion

The *L. infantum* LiGLO2 gene (GenBank accession No. DQ294972) was cloned and expressed in *E. coli* BL21 Codon Plus cells. The protein was expressed with an N-terminal His-tag fusion. A nickel-affinity column was used for purification. The purity of the recombinant *L. infantum* His-glyoxalase II was ≥95% as estimated by SDS-PAGE, which showed a single band corresponding to a molecular weight of about 32 kDa.

After optimization of the crystal-growth process, the purified protein produced thick plate crystals within 2 d (Fig. 1) which diffracted beyond 2.15 Å resolution using synchrotron radiation. The crystals belong to space group C222₁, with unit-cell parameters *a* = 65.7, *b* = 88.3, *c* = 85.2 Å. The calculated Matthews coefficient is 1.88 Å³ Da⁻¹, corresponding to a solvent content of ~35%, assuming the presence of one molecule in the asymmetric unit (Matthews, 1968). Data-collection and processing statistics are shown in Table 1.

Molecular replacement was performed using the human glyoxalase II structure (Cameron *et al.*, 1999; PDB code 1qh3; the full model was used), which shows 35% sequence identity with the *L. infantum* glyoxalase II, as a search model and the molecular-replacement program *Phaser* (Read, 2001). One clear solution was obtained and the calculated phases were improved using *Pirate* (Cowtan, 2000). A preliminary *C_α* trace was manually built from the search model and is currently being rebuilt using *COOT* (Emsley & Cowtan, 2004) and refined with *REFMAC5* from the *CCP4* suite (Collaborative Computational Project, Number 4, 1994).

The structure of *L. infantum* glyoxalase II, together with complete biochemical studies, will provide important insights into the molecular basis of trypanothione specificity.

The authors would like to thank the beamline staff at ID14-1 for assistance during data collection at the ESRF, Grenoble, France. This work was supported by projects POCTI/ESP/48272/2002 and BPD-9444/2002 (JT) from the Fundação para a Ciência e Tecnologia, Ministério da Ciência e Tecnologia, Portugal.

References

- Cameron, A. D., Ridderstrom, M., Olin, B. & Mannervik, B. (1999). *Structure*, **7**, 1067–1078.
- Collaborative Computational Project, Number 4 (1994). *Acta Cryst.* **D50**, 760–763.
- Cowtan, K. (2000). *Acta Cryst.* **D56**, 1612–1621.
- Emsley, P. & Cowtan, K. (2004). *Acta Cryst.* **D60**, 2126–2132.
- Fairlamb, A. H. & Cerami, A. (1992). *Annu. Rev. Microbiol.* **46**, 695–729.
- Hannaert, V., Saavedra, E., Duffieux, F., Szikora, J. P., Rigden, D. J., Michels, P. A. & Opperdoes, F. R. (2003). *Proc. Natl Acad. Sci. USA*, **100**, 1067–1071.
- Irsch, T. & Krauth-Siegel, R. L. (2004). *J. Biol. Chem.* **279**, 22209–22217.
- Leslie, A. G. W. (1992). *Jnt CCP4/ESF-EACBM Newsl. Protein Crystallogr.* **26**.
- Matthews, B. W. (1968). *J. Mol. Biol.* **33**, 491–497.
- Muller, S., Liebau, E., Walter, R. D. & Krauth-Siegel, R. L. (2003). *Trends Parasitol.* **19**, 320–328.
- Oza, S. L., Ariyanayagam, M. R., Aitchison, N. & Fairlamb, A. H. (2003). *Mol. Biochem. Parasitol.* **131**, 25–33.
- Read, R. J. (2001). *Acta Cryst.* **D57**, 1373–1382.
- Sousa Silva, M., Ferreira, A. E., Tomas, A. M., Cordeiro, C. & Ponces Freire, A. (2005). *FEBS J.* **272**, 2388–2398.